Hybrid stars with color superconductivity within a nonlocal chiral quark model

H. Grigorian*
Fachbereich Physik, Universität Rostock, D-18051 Rostock, Germany,
and Department of Physics, Yerevan State University, 375025 Yerevan, Armenia

D. Blaschke†
Fachbereich Physik, Universität Rostock, D-18051 Rostock, Germany,
and Bogoliubov Laboratory of Theoretical Physics, Joint Institute for Nuclear Research,
141980 Dubna, Moscow Region, Russia

D. N. Aguilera‡
Fachbereich Physik, Universität Rostock, D-18051 Rostock, Germany,
and Instituto de Física Rosario, Bv. 27 de febrero 210 bis, 2000 Rosario, Argentina
(Received 6 February 2004; published 23 June 2004)

The equation of state for quark matter is derived for a nonlocal, chiral quark model within the mean field approximation. Special emphasis is on the occurrence of a diquark condensate which signals a phase transition to color superconductivity and its effects on the equation of state. We present a fit formula for the Bag pressure, which is density dependent in the case when the quark matter is color superconducting. We calculate the quark star configurations by solving the Tolman-Oppenheimer-Volkoff equations and demonstrate the effects of diquark condensation on the stability of hybrid stars for different form factors of the quark interaction.

DOI: 10.1103/PhysRevC.69.065802 PACS number(s): 26.60.+c, 04.40.Dg, 12.38.Mh, 97.60.Jd

I. INTRODUCTION

The investigation of color superconductivity in quark matter [1,2] which was revived by applying nonperturbative QCD motivated interactions [3,4] finds most of its justification in the possible importance for the physics of compact star interiors [5] and related observable phenomena like neutron star cooling [6–8], gamma-ray bursts [9–12], gravitational wave signals for compact stars mergers [13] and others [14]. Since calculations of quark pairing predict values of the energy gap $\Delta \sim 100$ MeV and corresponding critical temperatures for the phase transition to the superconducting state are expected to follow the BCS relation $T_c = 0.57\,\Delta$ for spherical wave pairing, quark matter in compact stars should always be in one of the superconducting phases.

The question arises whether conditions in compact stars allow the occurence of quark matter and the formation of stable configurations of hybrid stars. In order to give an answer to this question one must rely on models for the equation of state which necessarily introduce free parameters and therefore some arbitrariness in the results [15]. In particular, the question whether color superconductivity shall be realized in the 2-flavor superconductivity (2SC) or color flavor locking (CFL) phase in the compact star interior has been discussed controversely [16,17]. We will restrict our further discussion to dynamical models of the NJL type with their parameters adjusted by fitting hadron properties in the vacuum before extrapolating to finite temperatures and densities within the Matsubara formalism.

Within those models it has been shown that strange quark matter occurs only at densities well above the deconfinement transition, for chemical potentials which are barely reached in the very center of a compact star [18–22]. The interesting and much investigated CFL phase could thus play only a marginal role for the physics of compact stars. The stability of the so obtained hybrid star configurations, however, appears to depend sensitively on details of the model, including the hadronic phase.

In the present paper we are investigating this dependence in a systematic way by employing a nonlocal chiral quark model which allows to vary the form factor of the interaction kernel while describing the same set of hadronic vacuum properties. We provide a polynomial fit formula of our quark matter equation of state (EoS) which proves useful for applications to compact star phenomenology as, e.g., the cooling [23] and rotational evolution [24] or the merging [13] of neutron stars. In order to compare the results of the present work for hybrid star configurations with observational constraints, we pick the example of the compact object RX J185635-3754, for which limits for both the mass and the radius have been reported [25,26]. A further restriction in the mass-radius plane of possible stable configurations comes from the constraint given by the surface redshift measurement of EXO 0748-676 [27].

II. EQUATION OF STATE OF HYBRID STAR MATTER IN β EQUILIBRIUM

A. Quark matter with color superconductivity

We consider the grand canonical thermodynamic potential for 2SC quark matter within a nonlocal chiral quark model

*Electronic address: hovik@darss.mpg.uni-rostock.de
†Electronic address: david.blaschke@physik.uni-rostock.de
‡Electronic address: deborah@darss.mpg.uni-rostock.de

TABLE I. Parameter sets (Λ, G_1, m) of the nonlocal chiral quark model for different form factors discussed in the text. The last three columns show the critical temperatures at vanishing chemical potential and the critical chemical potentials with and without diquark condensate at vanishing temperature, respectively.

Form factor	Λ(GeV)	$G_1\,\Lambda^2$	m(MeV)	$T_c(\mu=0)$(MeV)	$\mu_c^{(S)}(T=0)$(MeV)	$\mu_c^{(N)}(T=0)$(MeV)
Gaussian	1.025	3.7805	2.41	174	965	991
Lorentzian	0.8937	2.436	2.34	188	999	1045
NJL	0.9	1.944	5.1	212	1030	1100

[12] where in the mean-field approximation the mass gap ϕ_f and the diquark gap Δ appear as order parameters and a decomposition into color $(c \in \{r,b,g\})$ and flavor $(f \in \{u,d\})$ degrees of freedom can be made,

$$\Omega_q(\{\phi_f\},\Delta;\{\mu_{fc}\},T) = \sum_{c,f} \Omega^{c,f}(\phi_f,\Delta;\mu_{fc},T), \tag{1}$$

where T is the temperature and μ_{fc} the chemical potential for the quark with flavor f and color c.

The contribution of quarks with given color c and flavor f to the thermodynamic potential is

$$\Omega^{c,f}(\phi_f,\Delta;\mu_{fc},T) + \Omega^c_{\rm vac} = \frac{\phi_f^2}{24\,G_1} + \frac{\Delta^2}{24\,G_2} - \frac{1}{\pi^2} \times \int_0^\infty dq\; q^2\{\omega[\epsilon_c(E_f(q)+\mu_{fc}),T] + \omega[\epsilon_c(E_f(q)-\mu_{fc}),T]\}, \tag{2}$$

where G_1 and G_2 are coupling constants in the scalar meson and diquark channels, respectively. The dispersion relation for unpaired quarks with dynamical mass function $m_f(q) = m_f + g(q)\phi_f$ is given by

$$E_f(q) = \sqrt{q^2 + m_f^2(q)}. \tag{3}$$

In Eq. (2) we have introduced the notation

$$\omega[\epsilon_c,T] = T\,\ln\left[1+\exp\left(-\frac{\epsilon_c}{T}\right)\right] + \frac{\epsilon_c}{2}, \tag{4}$$

where the first argument is given by

$$\epsilon_c(\xi) = \xi\sqrt{1+\Delta_c^2/\xi^2}. \tag{5}$$

When we choose the green and blue colors to be paired and the red ones to remain unpaired, we have

$$\Delta_c = g(q)\Delta(\delta_{c,b}+\delta_{c,g}). \tag{6}$$

For a homogeneous system in equilibrium, the minimum of the thermodynamic potential Ω_q with respect to the order parameters $\{\phi_f\}$ and Δ corresponds to a negative pressure; therefore the constant $\Omega_{\rm vac} = \Sigma_c \Omega^c_{\rm vac}$ is chosen such that the pressure of the physical vacuum vanishes.

The nonlocality of the interaction between the quarks in both channels $q\bar{q}$ and qq is implemented via the same form-factor functions $g(q)$ in the momentum space. In our calculations we use the Gaussian (G), Lorentzian (L) and cutoff (NJL) type form factors defined as

$$g_{\rm G}(q) = \exp(-q^2/\Lambda_{\rm G}^2), \tag{7}$$

$$g_{\rm L}(q) = [1+(q/\Lambda_{\rm L})^2]^{-1}, \tag{8}$$

$$g_{\rm NJL}(q) = \theta(1-q/\Lambda_{\rm NJL}). \tag{9}$$

The parameter sets (quark mass m, coupling constant G_1, interaction range Λ) for the above form-factor models (see Table I) are fixed by the pion mass $m_\pi = 140$ MeV, pion decay constant $f_\pi = 93$ MeV, and the constituent quark mass $m_0 = 330$ MeV at $T = \mu = 0$ [32,33]. The diquark coupling constant G_2 is a free parameter of the approach which we vary as $G_2 = \eta\, G_1$.

Following Ref. [28] we introduce the quark chemical potential for the color c, μ_{qc} and the chemical potential of the isospin asymmetry, μ_I, defined as

$$\mu_{qc} = (\mu_{uc} + \mu_{dc})/2, \tag{10}$$

$$\mu_I = (\mu_{uc} - \mu_{dc})/2, \tag{11}$$

where the latter is color independent.

The diquark condensation in the 2SC phase induces a color asymmetry which is proportional to the chemical potential μ_8. Therefore we can write

$$\mu_{qc} = \mu_q + \frac{\mu_8}{3}(\delta_{c,b}+\delta_{c,g}-2\delta_{c,r}), \tag{12}$$

where μ_q and μ_8 are conjugate to the quark number density and the color charge density, respectively.

As has been shown in Ref. [29] for the 2SC phase the relation $\phi_u = \phi_d = \phi$ holds so that the quark thermodynamic potential is [30]

$$\Omega_q(\phi,\Delta;\mu_q,\mu_I,\mu_8,T)+\Omega_{\rm vac}=\frac{\phi^2}{4G_1}+\frac{\Delta^2}{4G_2}-\frac{1}{\pi^2}\int_0^\infty dqq^2\Bigg\{\omega\Big[\epsilon_r\Big(-\mu_q+\frac{2}{3}\mu_8-\mu_I\Big),T\Big]+\omega\Big[\epsilon_r\Big(\mu_q-\frac{2}{3}\mu_8-\mu_I\Big),T\Big]+\omega\Big[\epsilon_r\Big(-\mu_q+\frac{2}{3}\mu_8+\mu_I\Big),T\Big]+\omega\Big[\epsilon_r\Big(\mu_q-\frac{2}{3}\mu_8+\mu_I\Big),T\Big]\Bigg\}$$
$$-\frac{2}{\pi^2}\int_0^\infty dqq^2\Bigg\{\omega\Big[\epsilon_b\Big(E(q)-\mu_q-\frac{1}{3}\mu_8\Big)-\mu_I,T\Big]+\omega\Big[\epsilon_b\Big(E(q)+\mu_q+\frac{1}{3}\mu_8\Big)-\mu_I,T\Big]+\omega\Big[\epsilon_b\Big(E(q)-\mu_q-\frac{1}{3}\mu_8\Big)+\mu_I,T\Big]+\omega\Big[\epsilon_b\Big(E(q)+\mu_q+\frac{1}{3}\mu_8\Big)+\mu_I,T\Big]\Bigg\}, \quad (13)$$

where the factor 2 in the last integral comes from the degeneracy of the blue and green colors ($\epsilon_b=\epsilon_g$).

The total thermodynamic potential Ω contains besides the quark contribution Ω_q also that of the leptons $\Omega^{\rm id}$,

$$\Omega(\phi,\Delta;\mu_q,\mu_I,\mu_8,\mu_l,T)=\Omega_q(\phi,\Delta;\mu_q,\mu_I,\mu_8,T)+\sum_{l\in\{e,\bar{\nu}_e,\nu_e\}}\Omega^{\rm id}(\mu_l,T), \quad (14)$$

where the latter are assumed to be a massless, ideal Fermi gas

$$\Omega^{\rm id}(\mu,T)=-\frac{1}{12\pi^2}\mu^4-\frac{1}{6}\mu^2T^2-\frac{7}{180}\pi^2T^4. \quad (15)$$

At the present stage, we do include only contributions of the first family of leptons in the thermodynamic potential.

The conditions for the local extremum of Ω_q correspond to coupled gap equations for the two order parameters ϕ and Δ,

$$\left.\frac{\partial\Omega}{\partial\phi}\right|_{\phi=\phi_0,\Delta=\Delta_0}=\left.\frac{\partial\Omega}{\partial\Delta}\right|_{\phi=\phi_0,\Delta=\Delta_0}=0. \quad (16)$$

The global minimum of Ω_q represents the state of thermodynamic equilibrium from which all equations of state can be obtained by derivation.

B. Beta equilibrium, charge and color neutrality

The stellar matter in equilibrium has to obey the constraints of β-equilibrium ($d\to u+e^-+\bar{\nu}_e, u+e^-\to d+\nu_e$), expressed as

$$\mu_{dc}=\mu_{uc}+\mu_e, \quad (17)$$

color and electric charge neutrality and baryon number conservation.

We use in the following, the electric charge density,

$$Q=\frac{2}{3}\sum_c n_{uc}-\frac{1}{3}\sum_c n_{dc}-n_e; \quad (18)$$

the baryon number density,

$$n_B=\frac{1}{3}\sum_{f,c} n_{fc}; \quad (19)$$

and the color number density,

$$n_8=\frac{1}{3}\sum_f (n_{fb}+n_{fg}-2n_{fr}). \quad (20)$$

The number densities n_j occuring on the right-hand sides of the above equations (18)–(20) are defined as derivatives of the thermodynamic potential (14) with respect to corresponding chemical potentials μ_j,

$$n_j=-\left.\frac{\partial\Omega}{\partial\mu_j}\right|_{\phi_0,\Delta_0;T,\{\mu_i,i\neq j\}}. \quad (21)$$

Here the index j stands for the particle species.

In order to express the Gibbs free enthalpy density G in terms of those chemical potentials which are conjugate to the conserved densities and to implement the β-equilibrium condition (17) we make the following algebraic transformations:

$$G=\sum_{f,c}\mu_{fc}n_{fc}+\mu_e n_e$$
$$=\frac{1}{3}\sum_c(3\mu_{qc}-\mu_I)(n_{dc}+n_{uc})-\mu_e Q$$
$$=\mu_B n_B+\mu_Q Q+\mu_8 n_8, \quad (22)$$

where we have defined the chemical potential $\mu_B=3\mu_q-\mu_I$ conjugate to the baryon number density n_B in the same way as $\mu_Q=-\mu_e$ is the chemical potential conjugate to Q and μ_8 to n_8. Then, the electric and color charge neutrality conditions read

$$Q=0, \quad (23)$$

$$n_8=0, \quad (24)$$

at given n_B. The solution of the gap equations (16) can be performed under these constraints.

The solution of the color neutrality condition shows that μ_8 is about 5–7 MeV in the region of relevant densities ($\mu_q\simeq 300$–500 MeV). Since μ_I is independent of μ_8 we consider $\mu_{qc}\simeq\mu_q$ ($\mu_8\simeq 0$) in the following calculations.

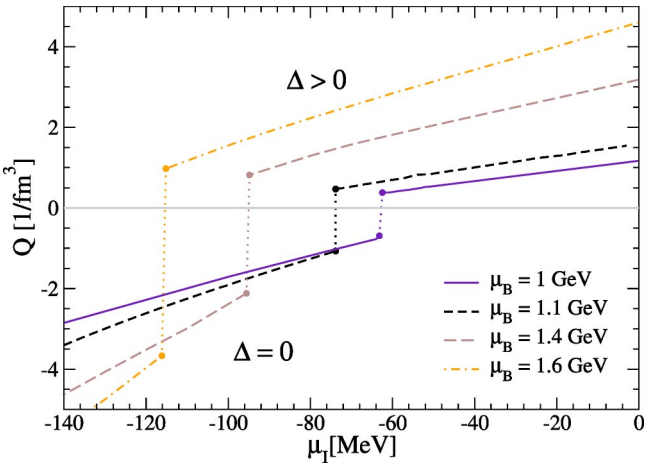

FIG. 1. (Color online) Electric charge density for the 2SC ($\Delta>0$) and normal ($\Delta=0$) quark matter phases as a function of μ_I for different fixed values of μ_B. The end points of the lines for given μ_B denote states with the same pressure and represent subphases in the Glendenning construction.

To demonstrate how to define a charge neutral state of quark matter in 2SC phase we plot in Fig. 1 the electric charge density Q as a function of μ_I for different fixed values of μ_B, when the system is in the global minimum of the thermodynamic potential and $\eta=1$. As has been shown before in Ref. [20] for the NJL model case, the pure phases ($\Delta>0$, superconducting; $\Delta=0$, normal) in general are charged. These branches end at critical values of μ_I where their pressure is equal and the corresponding states are degenerate

$$P = P_{\Delta=0}(\mu_B,\mu_I,\mu_e,T) = P_{\Delta>0}(\mu_B,\mu_I,\mu_e,T). \tag{25}$$

In order to fulfill the charge neutrality condition one can construct a homogeneous mixed phase of these states using the Gibbs conditions [31].

The volume fraction that is occupied by the subphase with diquark condensation is defined by the charges in the subphases

$$\chi = Q_{\Delta>0}/(Q_{\Delta>0} - Q_{\Delta=0}) \tag{26}$$

and is plotted in Fig. 2 for the different form-factor functions as a function of μ_B.

In the same way, the number densities for the different particle species j and the energy density are given by

$$n_j = \chi n_{j_{\Delta>0}} + (1-\chi) n_{j_{\Delta=0}}, \tag{27}$$

$$\varepsilon = \chi \varepsilon_{\Delta>0} + (1-\chi)\varepsilon_{\Delta=0}. \tag{28}$$

The formulas (25)–(28) define a complete set of thermodynamic relations and can be evaluated numerically. In the next section we present the results in a form analog to the Bag model which has been widely used in the phenomenology of quark matter.

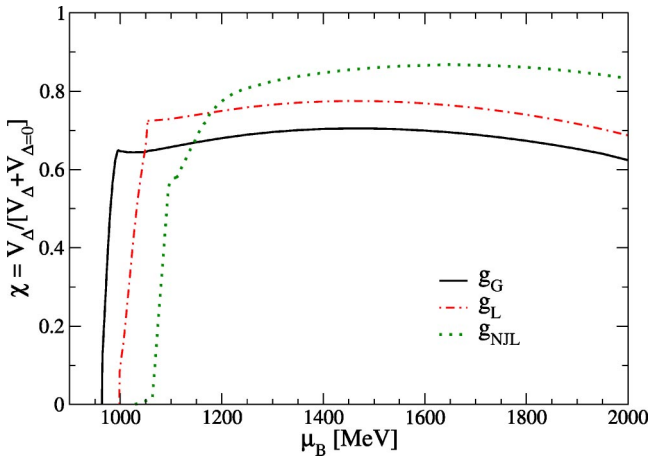

FIG. 2. (Color online) Volume fraction χ of the phase with nonvanishing diquark condensate obtained by a Glendenning construction of a charge-neutral mixed phase. Results are shown for three different form factors introduced in the text.

III. QUARK STAR EoS AND FIT FORMULAS

We calculate the quark matter EoS within this nonlocal chiral model [12] and display the results for the pressure in a form reminiscent of a bag model

$$P^{(s)} = P_{\rm id}(\mu_B) - B^{(s)}(\mu_B), \tag{29}$$

where $P_{\rm id}(\mu_B)$ is the ideal gas pressure of quarks and $B^{(s)}(\mu_B)$ a *density dependent* bag pressure, see Fig. 3. The occurrence of diquark condensation depends on the value of $\eta=G_2/G_1$ and the superscript $s\in\{S,N\}$ indicates whether we consider the matter in the superconducting mixed phase ($\eta=1$) or in the normal phase ($\eta=0$), respectively.

According to heuristic expectations, the effect of this diquark condensation (formation of quark Cooper pairs) on the EoS is similar to the occurrence of bound states and corresponds to a negative pressure contribution (Fig. 3).

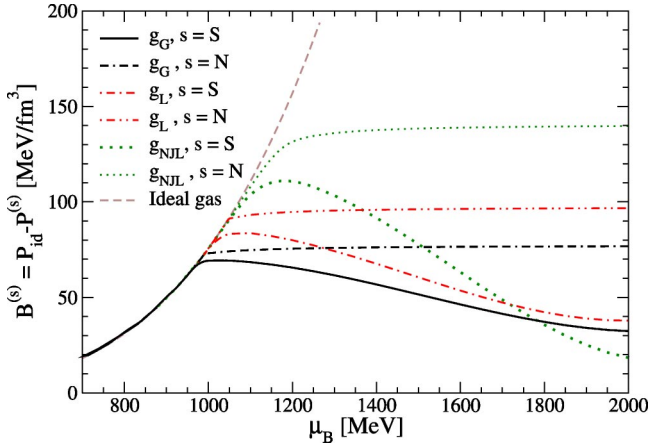

FIG. 3. (Color online) Bag pressure for different form factors of the quark interaction in dependence on the baryon chemical potential for $\eta=0$ and for $\eta=1$. For the latter the superconducting phase is realized.

TABLE II. Coefficients for the bag function fit formula for the normal phase case, for different form factors, Eq. (30).

	$a_k^{(N)}(\mathrm{GeV}^{1-k}\ \mathrm{fm}^{-3})$		
k	Gaussian	Lorentzian	NJL
0	7.2942×10^{-2}	9.0218×10^{-2}	1.1071×10^{-1}
1	2.5122×10^{-2}	7.6973×10^{-2}	3.0219×10^{-1}
2	-9.1152×10^{-2}	-6.8728×10^{-1}	$1.2820\times10^{+0}$
3	1.6402×10^{-1}	$3.7260\times10^{+0}$	$-4.0634\times10^{+1}$
4	-5.9621×10^{-3}	$-1.1862\times10^{+1}$	$3.0828\times10^{+2}$
5	-5.1899×10^{-1}	$2.2342\times10^{+1}$	$1.2301\times10^{+3}$
6	9.0892×10^{-1}	$-2.4464\times10^{+1}$	$2.9441\times10^{+3}$
7	-6.5617×10^{-1}	$1.4374\times10^{+1}$	$-4.3677\times10^{+3}$
8	1.7810×10^{-1}	$-3.5006\times10^{+0}$	$3.9376\times10^{+3}$
9	0	0	$-1.9774\times10^{+3}$
10	0	0	$4.2442\times10^{+2}$

For phenomenological applications of the quark matter EoS (29) we provide a polynomial fit of the bag pressure

$$B^{(s)}(\mu_B)=\begin{cases}\sum_{k=0}^{10} a_k^{(s)}(\mu_B-\mu_c^{(s)})^k, & \mu_B>\mu_c^{(s)},\\ P_{id}(\mu_B), & \mu_B<\mu_c^{(s)}.\end{cases} \tag{30}$$

The coefficients $a_k^{(s)}$ as well as the critical chemical potential $\mu_c^{(s)}$ of the chiral phase transition depend on the choice of the form factor (see Tables II and III).

The dependence of the diquark gap on the chemical potential can be represented in a similar way by the polynomial fit,

TABLE III. Coefficients for the bag function fit formula for the superconducting mixed phase, for different form factors, Eq. (30).

	$a_k^{(S)}(\mathrm{GeV}^{1-k}\ \mathrm{fm}^{-3})$		
k	Gaussian	Lorentzian	NJL
0	6.5168×10^{-2}	7.5350×10^{-2}	8.4897×10^{-2}
1	1.4638×10^{-1}	2.8766×10^{-1}	2.8604×10^{-1}
2	$-1.8020\times10^{+0}$	$3.2215\times10^{+0}$	$1.0708\times10^{+0}$
3	$9.8125\times10^{+0}$	$1.6528\times10^{+1}$	$-2.8157\times10^{+1}$
4	$-3.0515\times10^{+1}$	$-4.9352\times10^{+1}$	$1.6904\times10^{+2}$
5	$5.4888\times10^{+1}$	$8.7023\times10^{+1}$	$-5.4828\times10^{+2}$
6	$-5.6610\times10^{+1}$	$-8.9237\times10^{+1}$	$1.0896\times10^{+3}$
7	$3.1096\times10^{+1}$	$4.9210\times10^{+1}$	$-1.3643\times10^{+3}$
8	$-7.0479\times10^{+0}$	$-1.1275\times10^{+1}$	$1.0518\times10^{+3}$
9	0	0	$-4.5653\times10^{+2}$
10	0	0	$8.5443\times10^{+1}$

TABLE IV. Coefficients for the diquark condensate fit formula, for different form factors, Eq. (31).

	$b_k(\mathrm{GeV}^{1-k})$		
k	Gaussian	Lorentzian	NJL
0	9.33×10^{-2}	1.04×10^{-1}	3.30×10^{-2}
1	2.13×10^{-1}	1.63×10^{-1}	1.05×10^{0}
2	-4.27×10^{-2}	9.19×10^{-2}	-3.42×10^{0}
3	1.14×10^{-2}	-1.92×10^{-1}	6.13×10^{0}
4	-5.27×10^{-3}	8.88×10^{-2}	-5.20×10^{0}
5	0	0	1.55×10^{0}
6	0	0	1.03×10^{-1}

$$\Delta(\mu_B)=\begin{cases}\sum_{k=0}^{6} b_k(\mu_B-\mu_c^{(S)})^k, & \mu_B>\mu_c^{(S)},\\ 0, & \mu_B<\mu_c^{(S)},\end{cases} \tag{31}$$

where the coefficients b_k for the different form factors are given in Table IV.

The volume fraction also can be approximated by polynomials in the following form:

$$\chi(\mu_B)=\begin{cases}\sum_{k=0}^{6} c_k(\mu_B-\mu_c^{(\chi)})^k, & \mu_B>\mu_c^{(\chi)},\\ \sum_{k=0}^{1} c_k(\mu_B-\mu_c^{(S)})^k, & \mu_c^{(\chi)}>\mu_B>\mu_c^{(S)},\\ 0, & \mu_B<\mu_c^{(S)}.\end{cases} \tag{32}$$

The coefficients c_k and the chemical potentials $\mu_c^{(\chi)}$ are given in Table V for different form factors.

TABLE V. Coefficients for the volume fraction Eq. (32) and their valid ranges, for different form factors.

	$c_k(\mathrm{GeV}^{-k})$		
k	Gaussian	Lorentzian	NJL
$\mu_c^{(\chi)}$(MeV)	995	1054	1095
		For $\mu_c^{(S)}<\mu_B<\mu_c^{(\chi)}$	
0	1.29×10^{-1}	8.56×10^{-2}	7.00×10^{-3}
1	$1.66\times10^{+1}$	$1.15\times10^{+1}$	8.51×10^{0}
		For $\mu_c^{(\chi)}<\mu_B$	
0	6.28×10^{-1}	7.17×10^{-1}	5.60×10^{-1}
1	3.36×10^{-1}	2.83×10^{-1}	2.47×10^{0}
2	-3.94×10^{-1}	-3.43×10^{-1}	-7.67×10^{0}
3	6.57×10^{-2}	-1.19×10^{-2}	$1.06\times10^{+1}$
4	-8.78×10^{-3}	2.50×10^{-2}	-5.34×10^{0}
5	0	0	-6.25×10^{-1}
6	0	0	7.45×10^{-1}

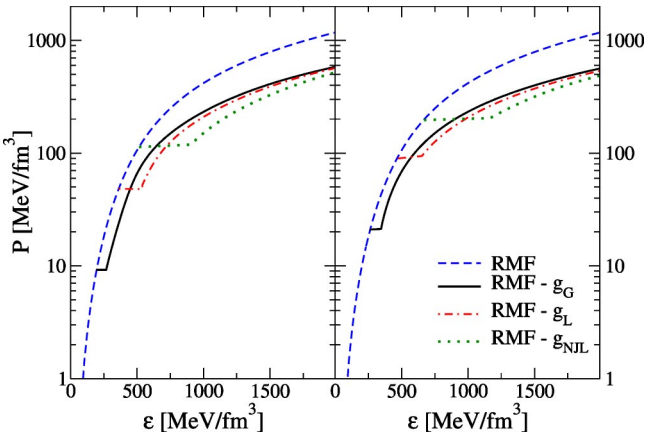

FIG. 4. (Color online) EoS for strongly interacting matter at zero temperature under compact stars constraints for the coupling parameter $\eta=1$ (left-hand panel) and $\eta=0$ (right-hand panel). Dashed line, relativistic mean-field model for hadronic matter; solid, dashed-dotted, and dotted lines correspond to quark matter with Gaussian, Lorentzian, and NJL form-factor functions, respectively.

IV. HADRONIC EQUATION OF STATE AND PHASE TRANSITION

At low densities, quarks will be confined in hadrons and an appropriate EoS for dense hadron matter must be chosen. For our discussion of quark-hadron hybrid star configurations in the next section, we use the relativistic mean field (RMF) model of asymmmetric nuclear matter including a nonlinear scalar field potential and the ρ meson (nonlinear Walecka model), see Ref. [34]. The quark-hadron phase transition is obtained using the Maxwell construction, see Refs. [35,36] for a discussion. The resulting EoS is shown in Fig. 4 for the case $\eta=1$ (left-hand panel) when the quark matter phase is superconducting and for $\eta=0$ (right-hand panel) when it is normal.

When comparing the three quark model form factors under consideration, the hardest quark matter EoS is obtained for the Gaussian, and therefore the critical pressure and corresponding critical energy densities of the deconfinement transition are the smallest, see Table II. The same statement holds for the case $\eta=0$, when the quark matter phases are normal, see right-hand panel of Fig. 4.

According to the Maxwell construction of the deconfinement phase transition, there is a jump in the energy density, as is shown in Fig. 4.

The corresponding jumps in the baryon densities at the critical chemical potentials $\mu_B^{(H)}$ are given in Table VI, see also Fig. 5 for the behavior of $n_B(\mu_B)$ for all three form factors and both cases of the diquark coupling, $\eta=1$ (left-hand panel) and $\eta=0$ (right-hand panel).

The EoS of hybrid stellar matter for temperature $T=0$ is relevant also for calculations of compact star cooling, since the star structure is insensitive to the temperature evolution for $T<1$ MeV.

V. CONFIGURATIONS OF HYBRID STARS

In this section we consider the problem of stability of cold ($T=0$) hybrid stars with color superconducting quark matter core. The star configurations are defined from the well-known Tolman-Oppenheimer-Volkoff equations [37], written for the hydrodynamical equilibrium of a spherically distributed matter fluid in general relativity, see also [34],

$$\frac{dP(r)}{dr} = -\frac{[\varepsilon(r)+P(r)][m(r)+4\pi r^3 P(r)]}{r[r-2m(r)]}, \tag{33}$$

where the mass enclosed in a sphere with distance r from the center of configurations is defined by

$$m(r) = 4\pi \int_0^r \varepsilon(r') r'^2 \, dr' . \tag{34}$$

These equations are solved for a set of central energy densities, see Figs. 6–9. An approximate criterion for the stability of star configurations is that masses should be rising functions of the central energy density $\varepsilon(0)$.

Our calculations show that for the Gaussian and Lorentzian form factors one can have stable configurations with a quark core, either with (Fig. 6) or without (Fig. 7) color superconductivity whereas for our parametrization of the

TABLE VI. Limiting densities of the coexistence region between quark (Q) and hadron (H) matter phases for different form factors ($n_0=0.16$ fm^{-3} is the nuclear saturation density) in the first two columns. The third column shows the critical baryon chemical potential at the phase transition $\mu_B^{(H)}=\mu_B^{(Q)}$, see Fig. 5. The subcolumns indicate the cases of superconducting ($\eta=1$) and normal ($\eta=0$) quark matter.

	$n_B^{(Q)}(n_0)$		$n_B^{(H)}(n_0)$		$\mu_B^{(H)}$(MeV)	
	$\eta=1$	$\eta=0$	$\eta=1$	$\eta=0$	$\eta=1$	$\eta=0$
Gaussian	1.84	2.14	1.20	1.68	1005	1059
Lorentzian	3.16	3.66	2.25	2.79	1149	1252
NJL	4.79	5.76	3.02	3.71	1303	1455

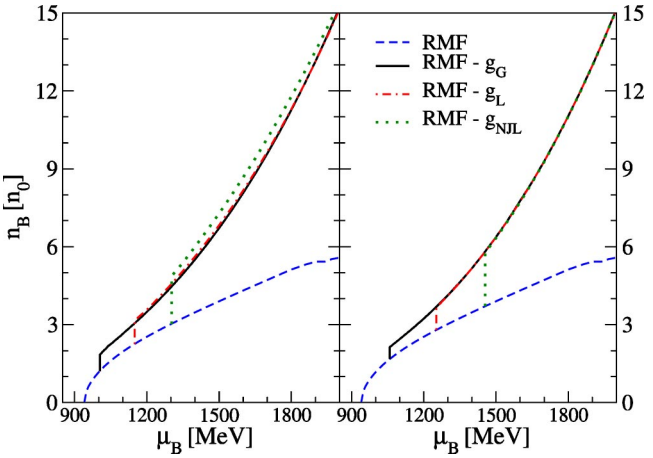

FIG. 5. (Color online) Baryon number density in units of the nuclear saturation density as a function of baryon chemical potential μ_B. Left-hand panel, $\eta=1$. Right-hand panel, $\eta=0$. Line styles correspond to the Fig. 4.

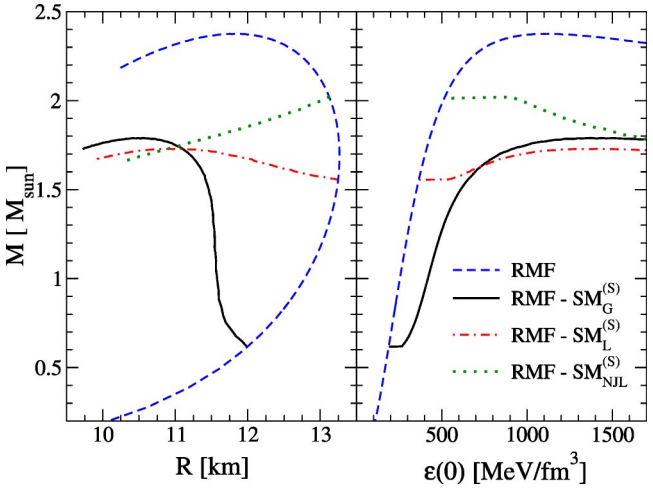

FIG. 6. (Color online) Mass-radius and mass-central energy density relation for compact stars configurations according to the EoS shown on the left-hand panel of Fig. 4. Hybrid stars with Gaussian or Lorentzian quark matter models give stable branches.

NJL model (cutoff form factor) the configurations with quark cores are not stable. For the Gaussian form-factor case the occurence of color superconductivity in quark matter shifts the critical mass of the hybrid star from $1.04M_{\odot}$ to $0.62M_{\odot}$ and the maximal value of the hybrid star mass from $1.83M_{\odot}$ to $1.79M_{\odot}$. For the Lorentzian form factor the branch of stable hybrid stars with 2SC supercondcting quark cores lies in the mass range between $1.55M_{\odot}$ and the maximum mass $1.72M_{\odot}$.

In Figs. 8 and 9 we demonstrate that these models fulfill the observational constraints from the isolated neutron star RX J185635-3754 [25,26] and from the observation of the surface redshift for EXO 0748-676 [27].

The Lorentzian model with normal quark matter has marginally stable quark cores with radii less than 2 km, in the mass range $1.91-1.92M_{\odot}$, see Fig. 9.

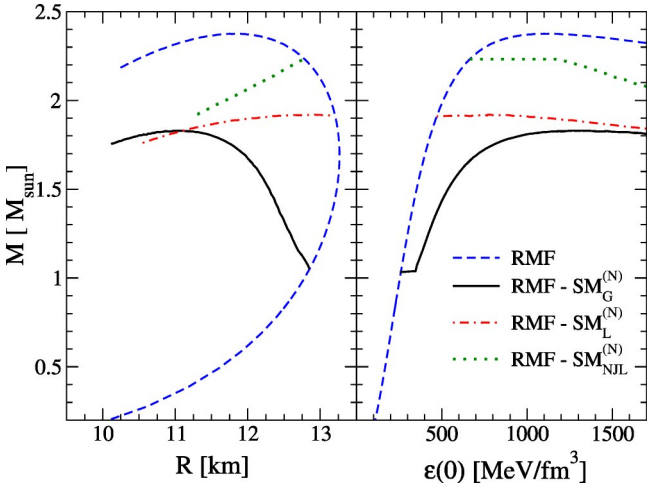

FIG. 7. (Color online) Same as Fig. 6 for the EoS of the right-hand panel of Fig. 4.

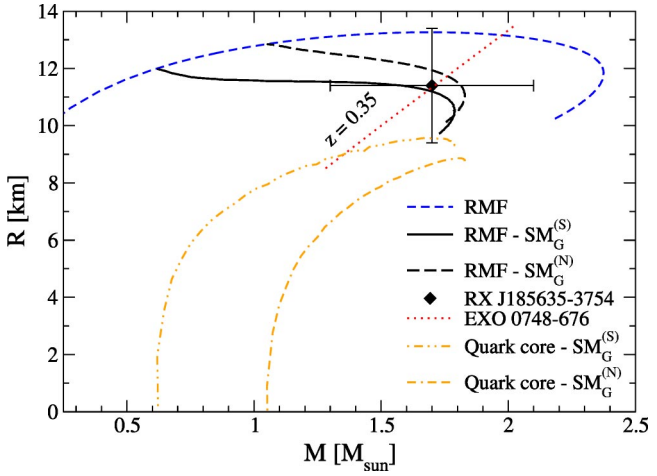

FIG. 8. (Color online) Radius-mass relation for Gaussian form factor including the mass dependence of the quark core radius in both cases, one with and the other without 2SC phase.

VI. CONCLUSION

We have investigated the influence of the diquark condensation on EoS of quark matter and obtained the critical densities of phase transition to hadronic matter for different form factors of quark interaction.

We find that the charge neutrality condition requires that the quark matter phase consists of a mixture of 2SC condensate and normal phase. The volume fraction of the condensate phase amounts to 65%–85% depending on the form-factor function of the interaction. In the present work we did not consider muons in the quark matter phase. Their occurence would increase the volume fraction of the superconducting phase by about 5%, helping to stabilize the 2SC phase.

We have shown that for our set of form factors the NJL model gives no stable quark core hybrid stars. The occurence of the superconducting 2SC phase in quark matter supports the stability of the quark matter phase.

Comparison of the quark core neutron star mass-radius relation with the mass and radius of the recently observed

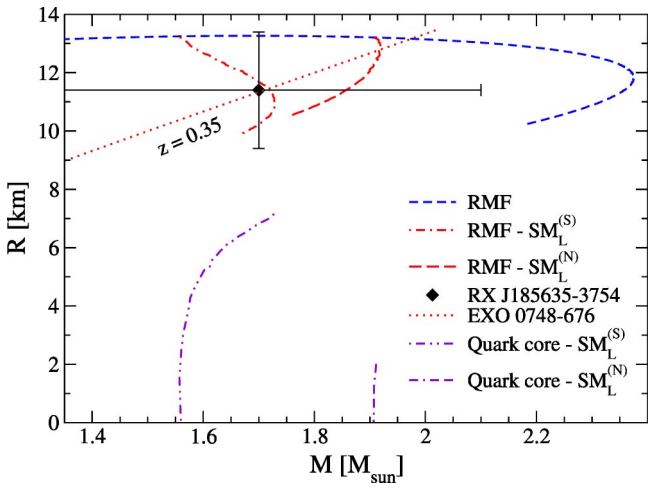

FIG. 9. (Color online) Same as Fig. 8 for Lorentzian form factor.

small compact object RX J185635−3754 and with the constraints from the observation of the surface redshift for the object EXO 0748-676 shows that our model perfectly obeys those constraints.

These studies can be viewed as a preparatory step before more fundamental nonperturbative interactions can be provided, e.g., by QCD Schwinger-Dyson equation studies [38–40].

ACKNOWLEDGMENTS

We thank our colleagues for discussions and interest in our work, in particular during the NATO workshop in Yerevan, Armenia. Special thanks to M. Buballa and D. Rischke for important remarks on a previous version of this work. The research of D.N. Aguilera has been supported by DFG Graduiertenkolleg 567 "Stark korrelierte Vielteilchensysteme," by CONICET PIP 03072 (Argentina), by DAAD Grant No. A/01/17862, by the Harms Stiftung of the University of Rostock, and by Landesgraduiertenfoerderung Mecklenburg-Vorpommern. H.G acknowledges support by DFG under Grant No. 436 ARM 17/5/01 and by the Virtual Institute of the Helmholtz Association "Dense Hadronic Matter and QCD Phase Transitions" under Grant No. VH-V1-041.

[1] B. C. Barrois, Nucl. Phys. **B129**, 390 (1977).
[2] D. Bailin and A. Love, Phys. Rep. **107**, 325 (1984).
[3] R. Rapp, T. Schafer, E. V. Shuryak, and M. Velkovsky, Phys. Rev. Lett. **81**, 53 (1998).
[4] M. Alford, K. Rajagopal, and F. Wilczek, Phys. Lett. B **450**, 325 (1999).
[5] D. Blaschke, N. K. Glendenning, and A. Sedrakian, *Physics Of Neutron Star Interiors*, Springer Lecture Notes in Physics 578 (Springer, New York, 2001).
[6] D. Blaschke, T. Klähn, and D. N. Voskresensky, Astrophys. J. **533**, 406 (2000).
[7] D. Page, M. Prakash, J. M. Lattimer, and A. Steiner, Phys. Rev. Lett. **85**, 2048 (2000).
[8] D. Blaschke, H. Grigorian, and D. N. Voskresensky, Astron. Astrophys. **368**, 561 (2001).
[9] D. K. Hong, S. D. H. Hsu, and F. Sannino, Phys. Lett. B **516**, 362 (2001).
[10] R. Ouyed, eConf C010815, 2002, p. 209.
[11] D. N. Aguilera, D. Blaschke, and H. Grigorian, Astron. Astrophys. **416**, 991 (2004).
[12] D. Blaschke, S. Fredriksson, H. Grigorian, and A. M. Öztas, Nucl. Phys. **A736**, 203 (2004).
[13] R. Oechslin, K. Uryu, G. Poghosyan, and F. K. Thielemann, Mon. Not. R. Astron. Soc. **349**, 1469 (2004).
[14] M. Alford, Annu. Rev. Nucl. Part. Sci. **51**, 131 (2001).
[15] M. Alford and S. Reddy, Phys. Rev. D **67**, 074024 (2003).
[16] M. Alford and K. Rajagopal, J. High Energy Phys. **0206**, 031 (2002).
[17] A. W. Steiner, S. Reddy, and M. Prakash, Phys. Rev. D **66**, 094007 (2002).
[18] C. Gocke, D. Blaschke, A. Khalatyan, and H. Grigorian, hep-ph/0104183.
[19] M. Buballa and M. Oertel, Nucl. Phys. **A703**, 770 (2002).
[20] F. Neumann, M. Buballa, and M. Oertel, Nucl. Phys. **A714**, 481 (2003).
[21] I. Shovkovy, M. Hanauske, and M. Huang, Phys. Rev. D **67**, 103004 (2003).
[22] M. Baldo, M. Buballa, F. Burgio, F. Neumann, M. Oertel, and H. J. Schulze, Phys. Lett. B **562**, 153 (2003).
[23] D. Blaschke, D. N. Voskresensky, and H. Grigorian, "Cooling evolution of hybrid stars with two-flavor color superconductivity," astro-ph/0403171.
[24] G. S. Poghosyan, H. Grigorian, and D. Blaschke, Astrophys. J. **551**, L73 (2001).
[25] M. Prakash, J. M. Lattimer, A. W. Steiner, and D. Page, Nucl. Phys. **A715**, 835 (2003).
[26] R. Turolla, S. Zane, and J. J. Drake, Astrophys. J. **603**, 265 (2004).
[27] J. Cottam, F. Paerels, and M. Mendez, Nature (London) **420**, 51 (2002).
[28] M. Huang, P. F. Zhuang, and W. Q. Chao, Phys. Rev. D **67**, 065015 (2003).
[29] M. Frank, M. Buballa, and M. Oertel, Phys. Lett. B **562**, 221 (2003).
[30] O. Kiriyama, S. Yasui, and H. Toki, Int. J. Mod. Phys. E **10**, 501 (2001).
[31] N. K. Glendenning, Phys. Rev. D **46**, 1274 (1992).
[32] S. M. Schmidt, D. Blaschke, and Y. L. Kalinovsky, Phys. Rev. C **50**, 435 (1994).
[33] J. Berges and K. Rajagopal, Nucl. Phys. **B538**, 215 (1999).
[34] N. K. Glendenning, *Compact Stars: Nuclear Physics, Particle Physics, and General Relativity* (Springer, New York, London, 2000).
[35] D. N. Voskresensky, M. Yasuhira, and T. Tatsumi, Phys. Lett. B **541**, 93 (2002).
[36] D. N. Voskresensky, M. Yasuhira, and T. Tatsumi, Nucl. Phys. **A723**, 291 (2003).
[37] J. R. Oppenheimer and G. M. Volkoff, Phys. Rev. **55**, 374 (1939).
[38] A. Bender, D. Blaschke, Y. Kalinovsky, and C. D. Roberts, Phys. Rev. Lett. **77**, 3724 (1996).
[39] C. D. Roberts and S. M. Schmidt, Prog. Part. Nucl. Phys. **45**, S1 (2001).
[40] A. Maas, B. Grüter, R. Alkofer, and J. Wambach, hep-ph/0210178.